Platinum Monolayer Electrocatalysts

Project FC141

PI: Jia Wang

Co-PIs: Kotaro Sasaki and Miomir Vukmirovic

Co-worker: Liang Song and Zhixiu Liang

Brookhaven National Laboratory

DOE Hydrogen and Fuel Cells Annual Merit Review
May 1, 2019

BROOKHAVEN
NATIONAL LABORATORY

Overview

Timeline

Start: September 2015
End: October 2019

Barriers

A. Catalysts' Durability:
< 40% loss in activity after 30,000 cycles
B. Catalysts' Performance:
Catalyst activity; ≥ 0.44 A/mg$_{PGM}$
C. Catalysts' Cost:
PGM loading; ≤ 0.125 mg PGM /cm^2

Budget

Funding received in
FY2018: $600,000
FY2019: $500,000

Collaborators

General Motors
Toyota M. C.
N.E. CHEMCAT Co.

Relevance

Project objective

Developing active, durable core-shell catalysts for the oxygen reduction reaction (ORR) that meet the DOE technical targets (Table3.4.7)
Activity at 0.9 V >0.44 A/mg_{PGM}, loss <40% after catalyst and support AST
<30 mV loss at 0.8 A/cm^2 after catalyst AST (30,000 cycles 0.6-0.95V)
<30 mV loss at 1.5 A/cm^2 after support AST (5,000 cycles 1-1.5V)

RDE screening targets

Activity >0.6 A/mg_{PGM} after catalyst AST (this period), including support AST (next goal). ECSA >40 m^2/g after catalyst AST.

Tasks and deliverables

- Innovate and validate new core materials, core-shell structures, and scalable synthesis methods for advancing cathode catalysts/support
- Deliver samples with performance exceeding RDE targets for MEA tests by collaborates

Status and impact

- Synthesis of active, durable **PtNiN** catalysts is improved based on better understanding of lattice structure and Pt segregation behavior.
- Nitride-stabilized bimetallic catalysts on suitable carbon supports are promising for >0.4 A/g activity after both catalyst and support ASTs.
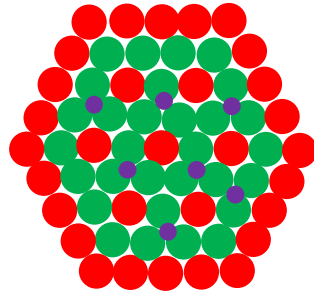
Approach
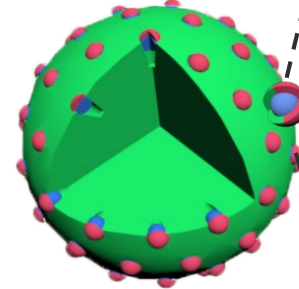
Two types of catalysts with low and PGM-free cores:

$Pt_{skin}(PtNi)_4N)_{core}$

Pt ●
Ni ●
N ●

Pt-NbO$_x$C nano-nail

Pt shells on top of **NbO$_x$** cores that are partly embedded in **carbon**

Bright dots for ordered **Pt** atoms in shell

Gray area for embedded amorphous **NbO$_x$** core

○ Ni is the best activity promoter for ORR, but is prone to dissolution in PEMFC.
○ Nitriding stabilizes Ni resulting in high ECSA, activity, and durability.

➢ Structural advantage of nitride core for stability of monolayer Pt skin catalyst clarified.
➢ Correlation of performance (ECSA, activity, and durability) with properties (Ni content, lattice phase, and Pt segregation) established.

○ Pt binds carbon weakly and catalyzes carbon corrosion, resulting in loss of carbon and ECSA after support AST.
○ Embedding NbO$_x$ in 4-nm pores on carbon and depositing Pt on top anchors down each of Pt half-shell particles, which minimizes particle agglomeration and carbon corrosion.

➢ Small effort in this period
➢ Future studies planned for enhancing support durability.

4

Tasks and Outline

Last year status: The best RDE results exceeded activity and durability targets, but MEA results have not met the two targets concurrently.

	Target	PtNiN			
		MEA			**RDE**
		GM#1	**LANL**	**GM#2**	**BNL**
MA (A mg^{-1})	> 0.44	0.37		0.15	0.91 / 0.5
MA loss (30K)	< 40%	-19%		-56%	-18%
ECSA (m^2/g)		27		44	89 / 50
ECSA loss	< 40%	-21%		-50%	-13%
Loss @0.8 Acm^{-2}	<30 mV	30	0	75	

Pt-NbO$_x$C		
MEA		**RDE**
UW	**GM**	**BNL**
0.12	0.03	0.56
		-4%
	20	66
	+25%	
No loss after support AST		

Before optimizing MEA fabrication for PtNiN, we need to better understand and optimize catalysts.

(1) XRD and TEM characterization for clarifying favorable PtNiN lattice structure and formation of Pt monolayer skin (slides #6-10)

(2) Intermetallic phase for PtNiN on porous Ketjenblack 300J (Slides #11-14)

Summary – RDE screen criteria (slide #15)

Oxidation of NbO$_x$ at higher temperature may be one of the causes of low MEA activity.

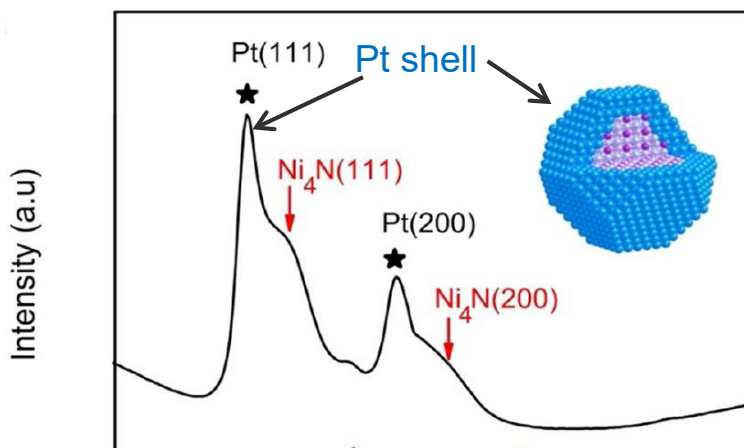(3) XPS and TEM results confirmed structural model. (Slide #16)
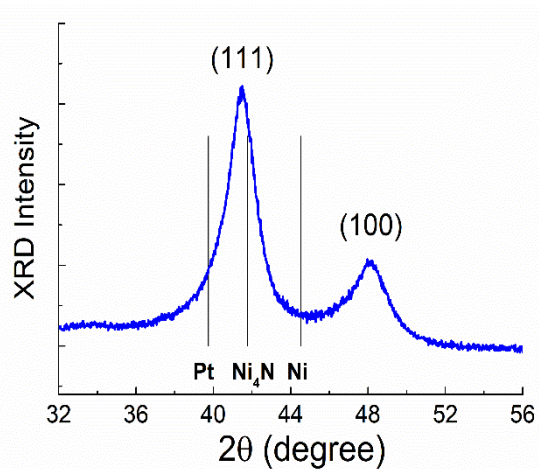
1a. Pt distribution: Core-shell or thin skin

Ni only

Core-shell structure has a Pt-only shell and a **Ni(N)-only core**.

Ni rich

Pt-skin structure also has a Pt-only shell, but with a PtNi(N)-**alloy(nitride) core**

Shoulder peaks indicate the lattice spacing of Ni$_4$N core is smaller than that of the 3-4 ML Pt shell.

A single set of symmetric peaks suggests uniform lattice spacing of alloy or a monolayer Pt skin

Pt$_{ML}$-(PtNi)$_4$N skin-core

Pt ●
Ni ●
N ●

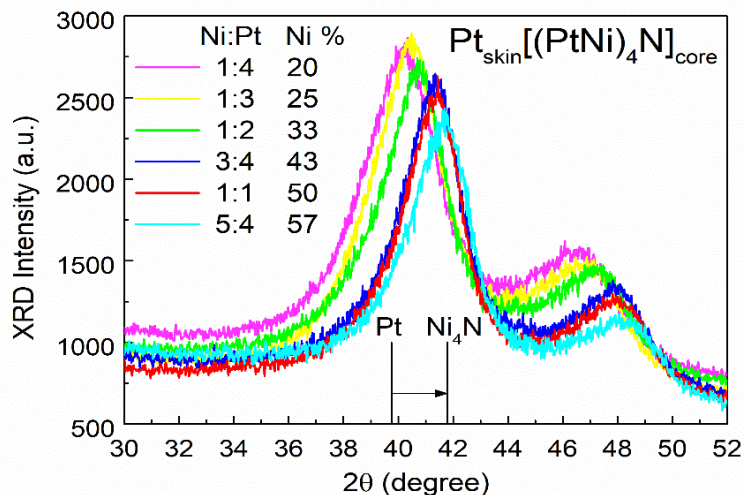Pt Monolayer can be commensurate with Ni-rich nitride core

---
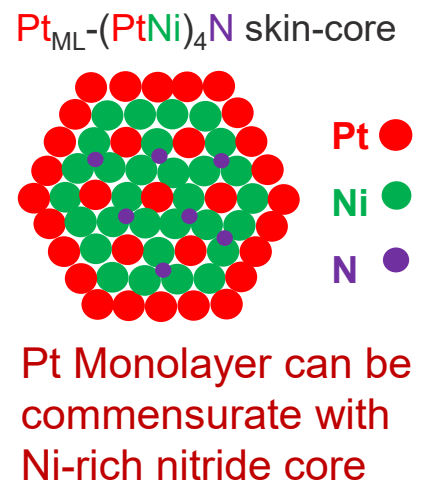
No need to de-alloy Ni in acid for both types of PtNiN catalysts. While similar ECSA can be obtained, a monolayer skin layer is favored for high activity enhancement by subsurface Ni.

How to characterize and optimize thin skin catalysts?
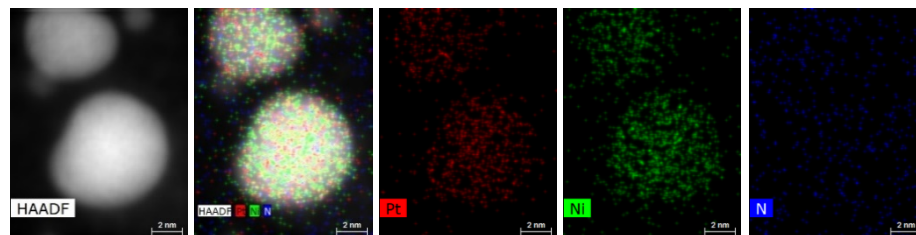
6

1b. Single-phase PtNiN with Ni% up to 57%
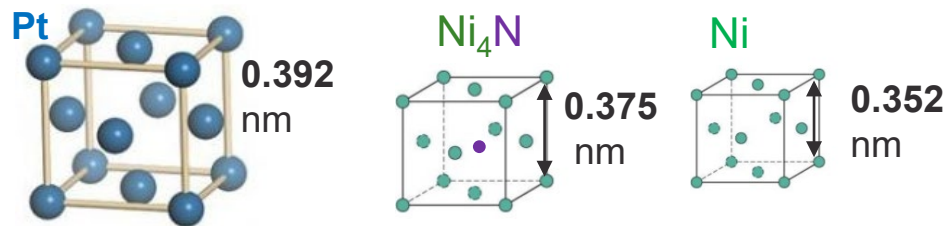
Ni$_4$N has one N atom at the center of FCC cubic cell, which expands Ni lattice resulting in a reduction of the lattice mismatch with Pt from **-10.2%** to **-4.6%**.

Moderate lattice mismatch between Pt and Ni$_4$N facilitates formation of single phase, stable PtNiN particles with high Ni content.
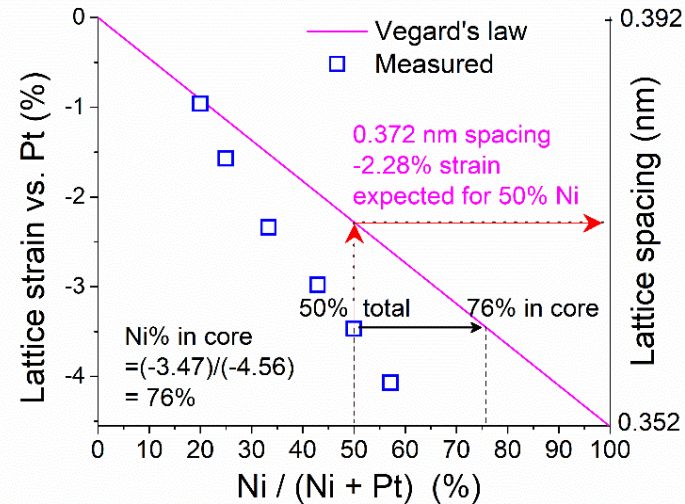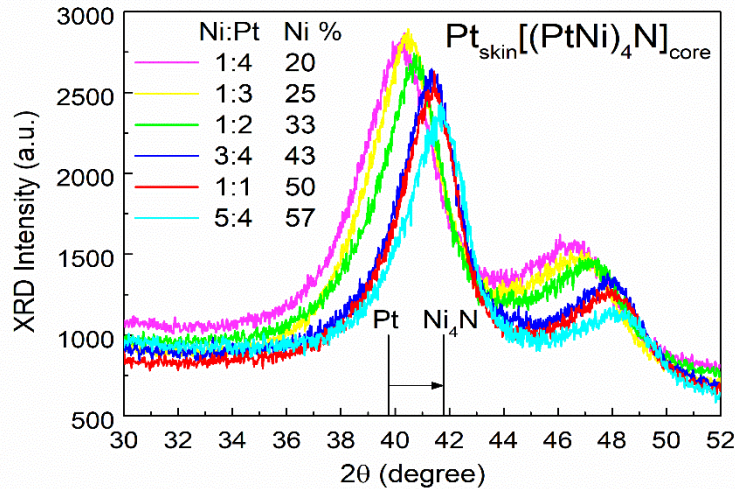

HAADF and EDS mappings of PtNiN particles (Pt:Ni 4:3) show single phase particles.
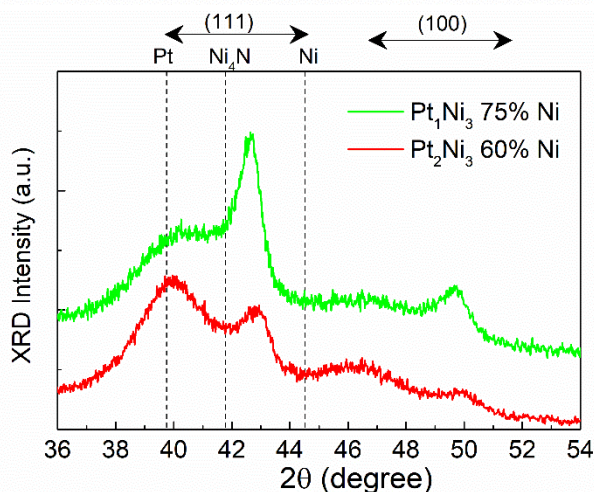
Phase separation occurs with 60% and 75% Ni for PtNiN.

Without Pt, Ni$_3$N forms.

Images of 2D projection can not tell whether there is a Pt skin layer of 1-2 monolayer thick

7

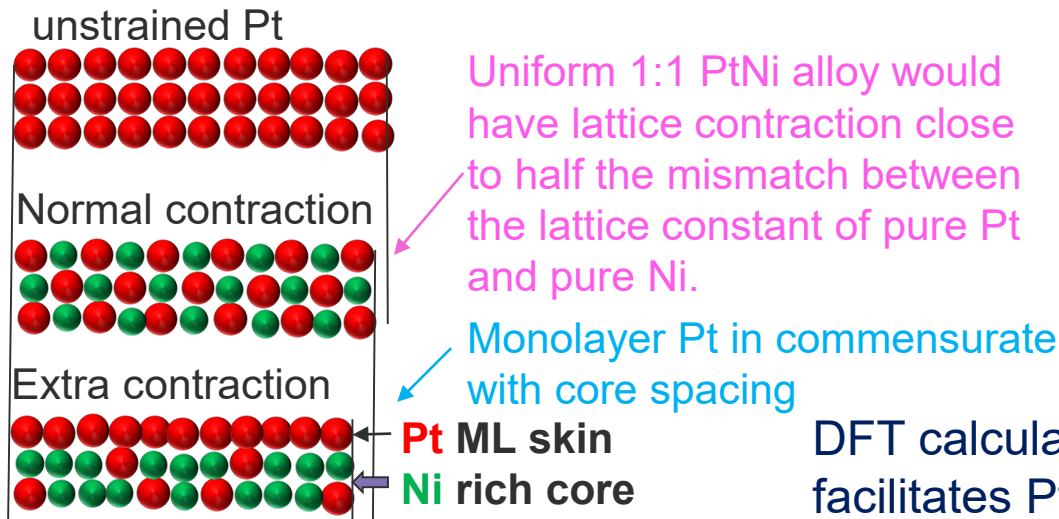# 1c. Contracted Pt ML skin on PtNiN cores

XRD peak shifts show lattice contraction increases with increasing Ni atomic %.

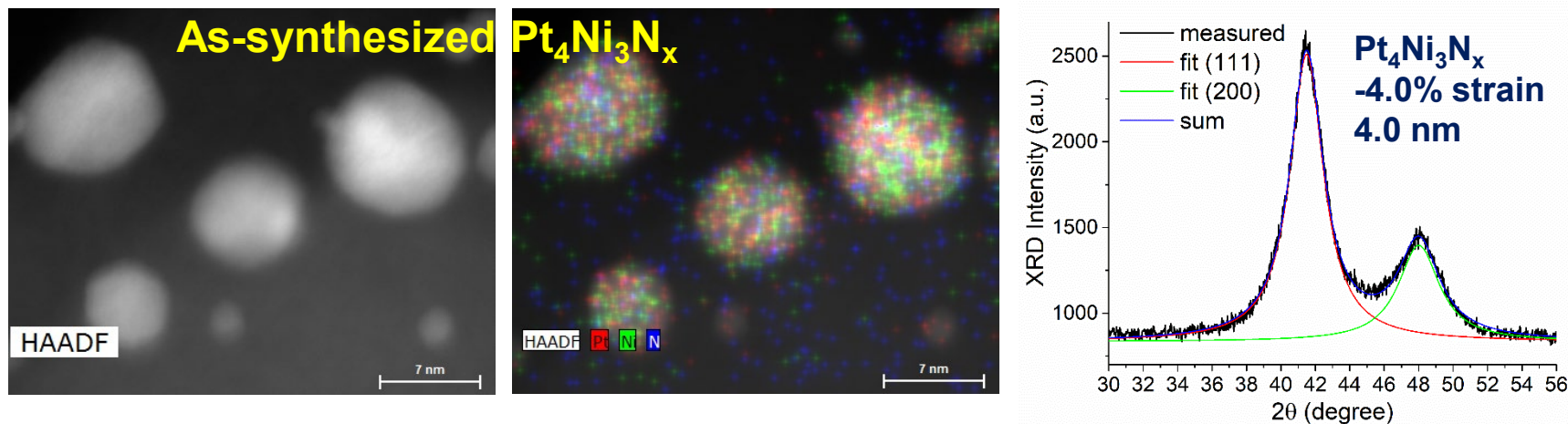Lattice strains (squares) are larger than expected by the linear relationship based on total Ni%.

Uniform 1:1 PtNi alloy would have lattice contraction close to half the mismatch between the lattice constant of pure Pt and pure Ni.

Monolayer Pt in commensurate with core spacing

Extra lattice contraction indicates formation of monolayer-like Pt skin layer on Ni-enriched alloy nitride cores.

DFT calculation supports that nitriding facilitates Pt segregation to surface

Kuttiyiel, Sasaki, Adzic, et al., *Nano Lett.*, 2012, 12, 6266

8

1d. HAADF and EDS of PtNiN on Vulcan

As-synthesized $Pt_4Ni_3N_x$

HAADF · HAADF · Pt · Ni · N · 7 nm

$Pt_4Ni_3N_x$
-4.0% strain
4.0 nm

After 30,000 cycles

HAADF · HAADF · Pt · Ni · N · 5 nm

HAADF and EDS mapping confirm even distribution of Pt, Ni, and N and single phase particles.
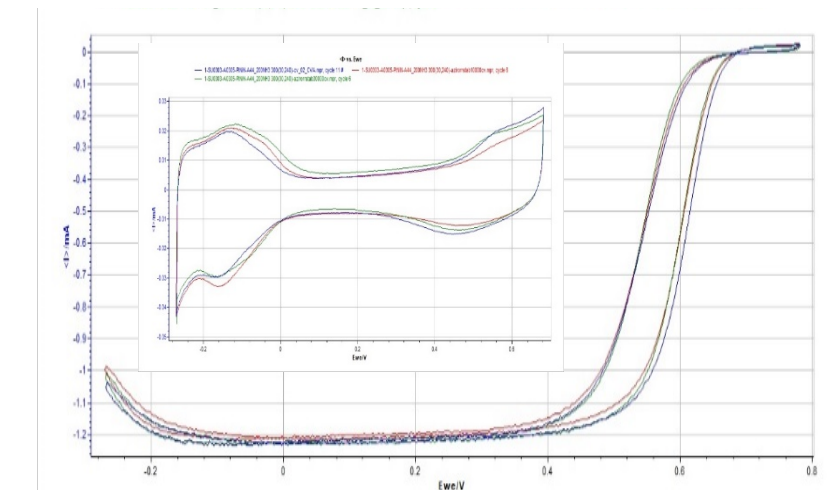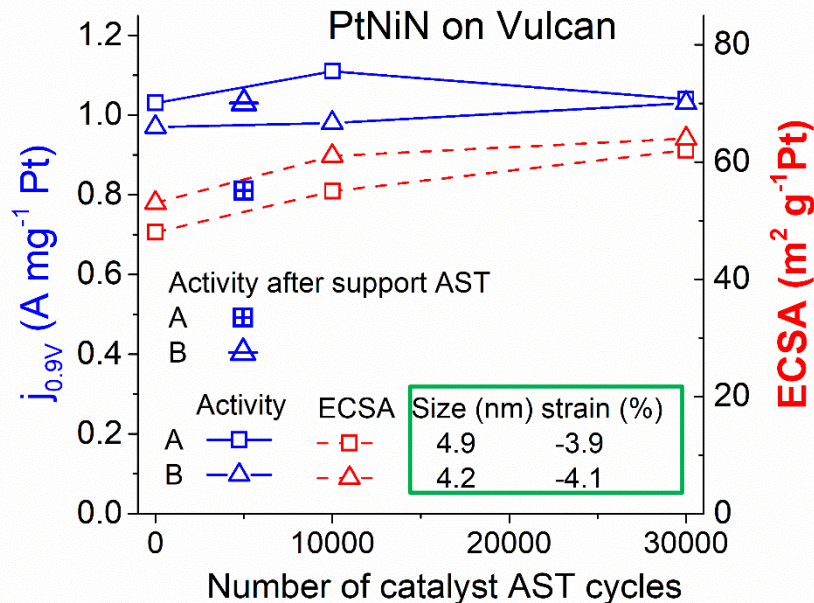
After catalyst AST, little change in particle size and element distribution.
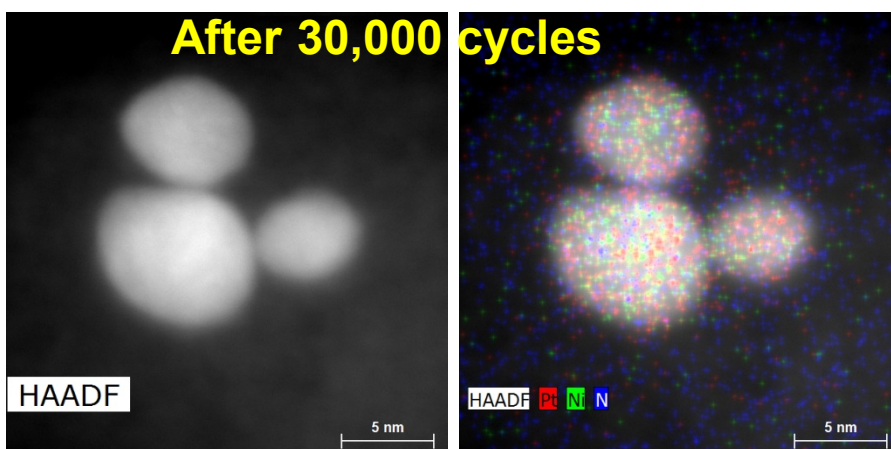
Formation of Pt monolayer skin layer on Ni-enriched nitride core leads to large lattice contraction (XRD) and high structural stability (TEM-EDS) , which enhance activity and durability of PtNiN catalysts.

9

1e. Performance of PtNiN on VC

PtNiN on Vulcan

Activity after support AST
A
B

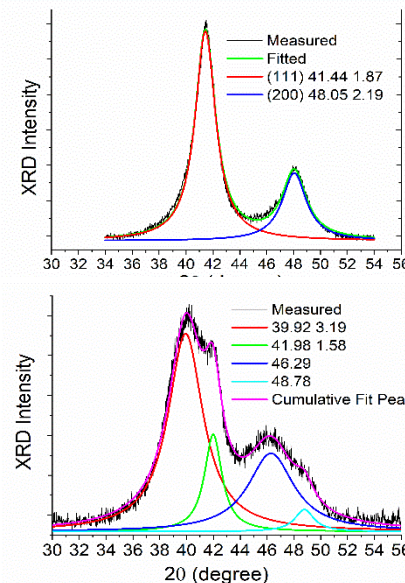|	Activity	ECSA	Size (nm)	strain (%)
A			4.9	-3.9
B			4.2	-4.1

A typical set of ORR and CV curves on RDE

# of cycles: 0 (blue), 10k (red), 30k (green)

Sample A has higher Pt wt% than B.
Both have Ni/(Ni+Pt) atomic% ~44%.

No loss of activity and durability after catalyst and support ASTs

Activity >0.8 A/mg, ECSA >50 m^2/g

Structure-performance correlation clarified but remains complicated and will be further tuned.


Samples having a single set of symmetric XRD peaks are far more active and durable than those having two sets of peaks because a thick Pt shell with little lattice contraction is less active and lattice mismatch at core-shell interface reduces structural stability.
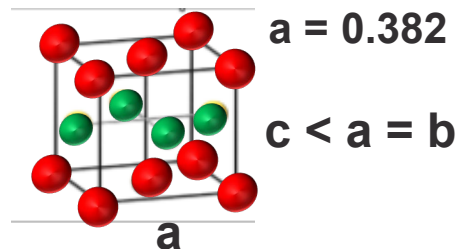
10

2a. PtNiN intermetallic on Ketjenblack 300J

Significantly improved activity and durability have been shown by long-range chemical ordered intermetallic, e.g., $L1_2$-Pt_3Co, **$L1_0$-Pt_1Co_1,** $L1_0$-Pt_1Ni_1
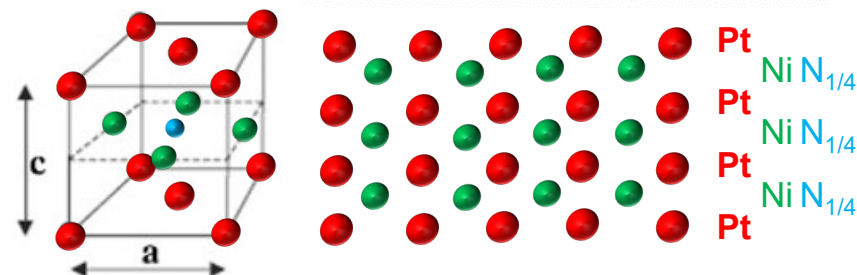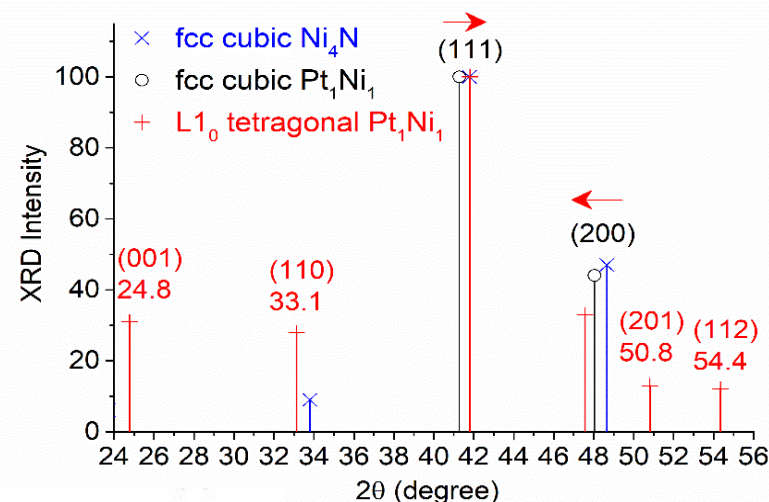
Regular alloy
c / a = 1.0
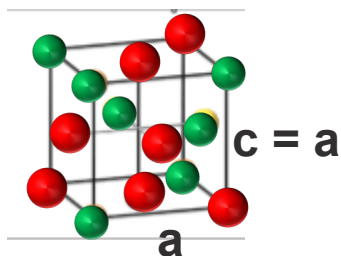
$L1_0$ Intermetallic
c / a = 0.94

c = 0.359 nm
a = 0.382 nm

c = a

a

c < a = b

a

Higher temperature and longer anneal time often cause too large particle size.

Ketjenblack EC-300J was used as support partly for keeping particles small during long nitriding time. Two sets of samples made: 510 ºC for **2–40** h and 560 ºC for **2–18** h.

× fcc cubic Ni_4N
○ fcc cubic Pt_1Ni_1
+ $L1_0$ tetragonal Pt_1Ni_1

XRD Intensity

(111)

(200)

(001) 24.8

(110) 33.1

(201) 50.8

(112) 54.4

2θ (degree)


Pt
Ni $N_{1/4}$
Pt
Ni $N_{1/4}$
Pt
Ni $N_{1/4}$
Pt

Similar XRD pattern expected for $L1_0$ Pt_1Ni_1N intermetallic; N at the center further stabilizes ordered structure. The x-y planes are alternately occupied by Pt and Ni atoms, causing a=b > c and thus (111) and (200) shift in opposite directions

11

2b. XRD of intermetallic PtNiN on KB
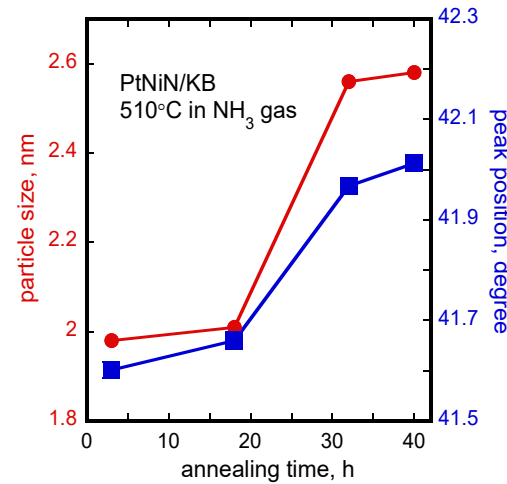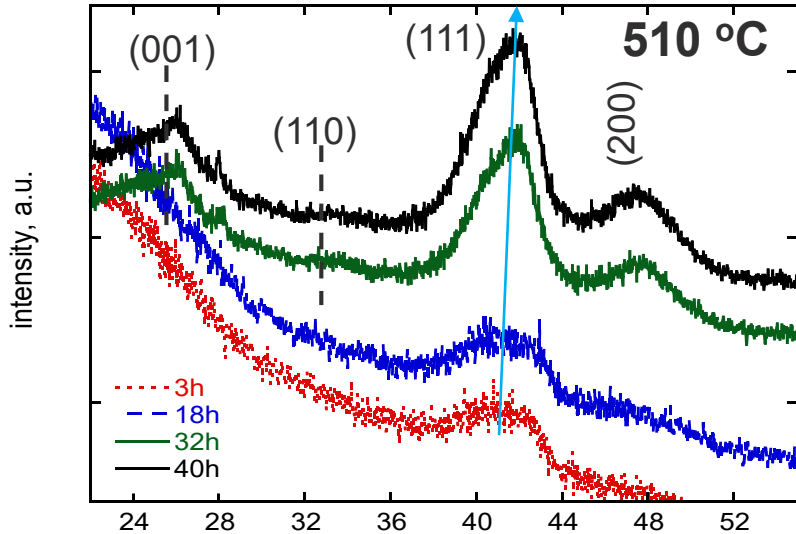
The (111) peak shifting to larger angle with increase of annealing time.
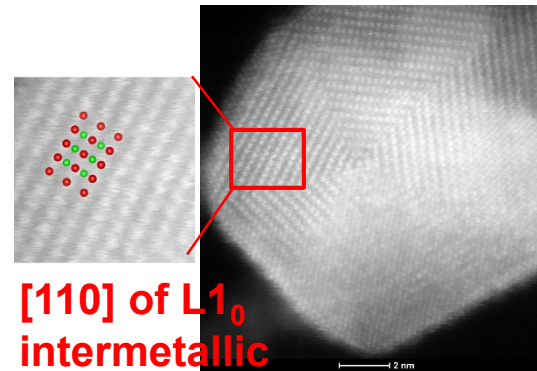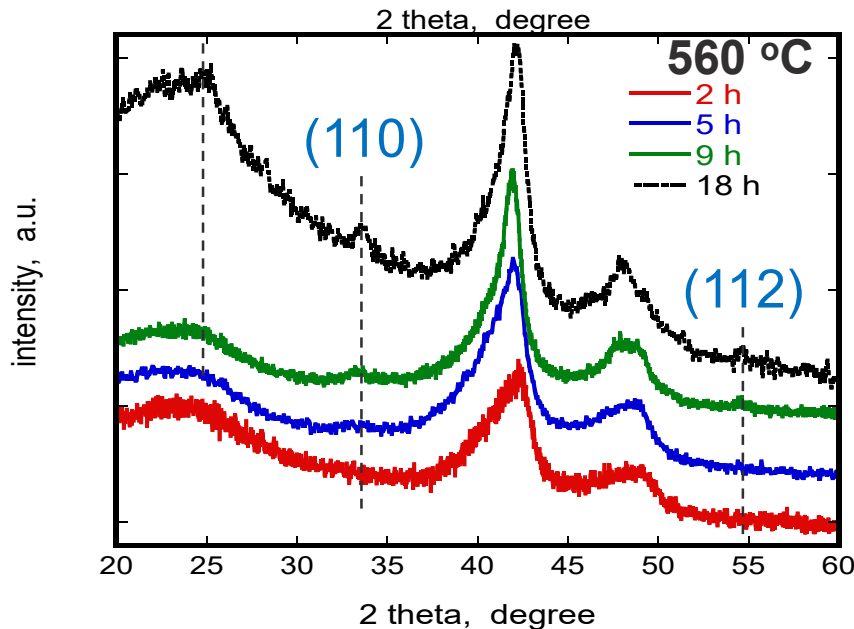
A high resolution image shows the [110] of $L1_0$ lattice spacing.

[110] of $L1_0$ intermetallic

(110) and (112) peaks emerged
(200) peak shifts to smaller angle

With total Pt:Ni 4:3, some particles form $L1_0$ Pt_2Ni_2N cores.

12

2c. EDS and TEM of PtNiN on KB (vs on VC)

PtNiN / KB 560ºC 9h

HAADF
Pt Ni N
3 nm

PtNiN/KB (560ºC, 9h) after 30k cycles

HAADF
Pt Ni N
4 nm
Pt Ni
4 nm

PtNiN on KB300 560 ºC 9h

2 nm
10 nm
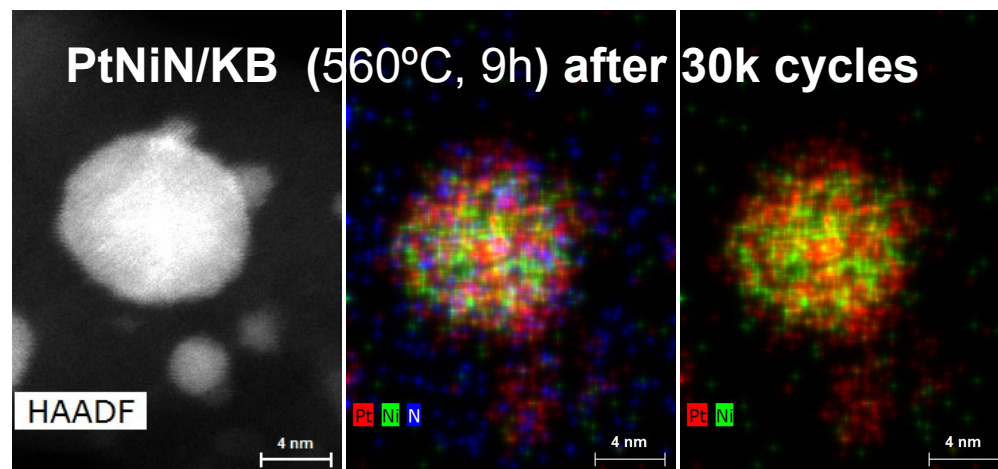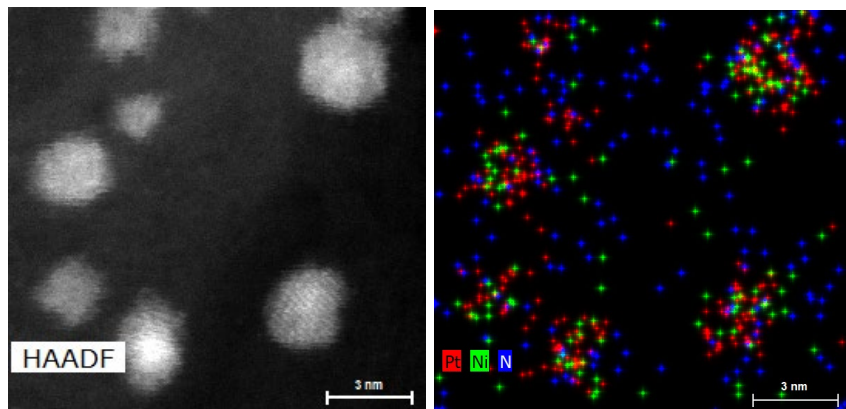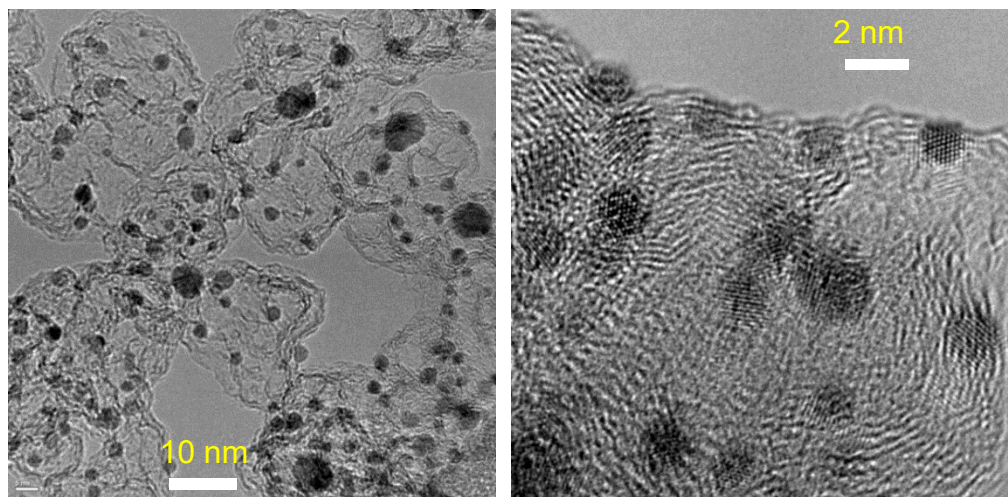
Many but not all embedded in graphitized carbon

PtNiN on VC 510 ºC 2h

20 nm
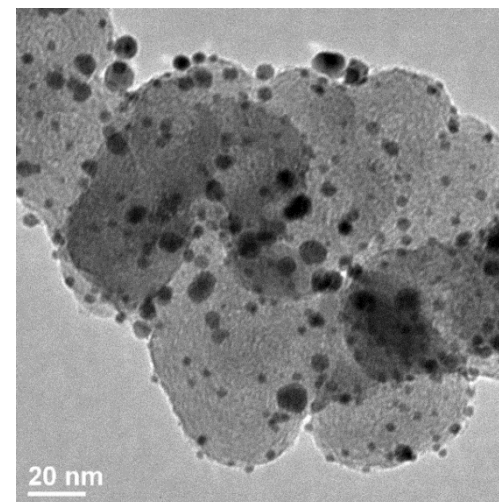
Most attached on surface

13

2d. ORR on RDE for intermetallic **PtNiN on KB** Accomplishment
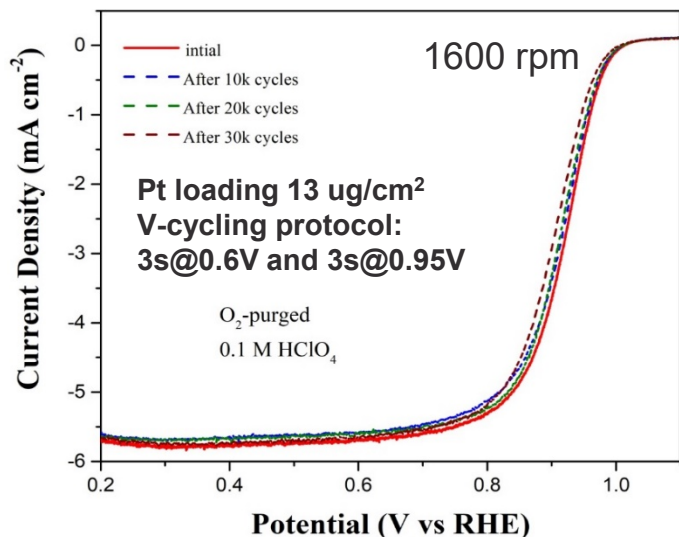
| | 560ºC 9h | | 510ºC 32h | |
V-cycle	MA (A/mg)	ECSA (m2/g)	MA (A/mg)	ECSA (m2/g)
0	1.20	61	0.59	58
10k	1.03	63	0.87	61
20k	0.98	60	0.56	61
30k	0.73 (-39%)	59 (-3%)	0.54 (-8%)	54 (-8%)
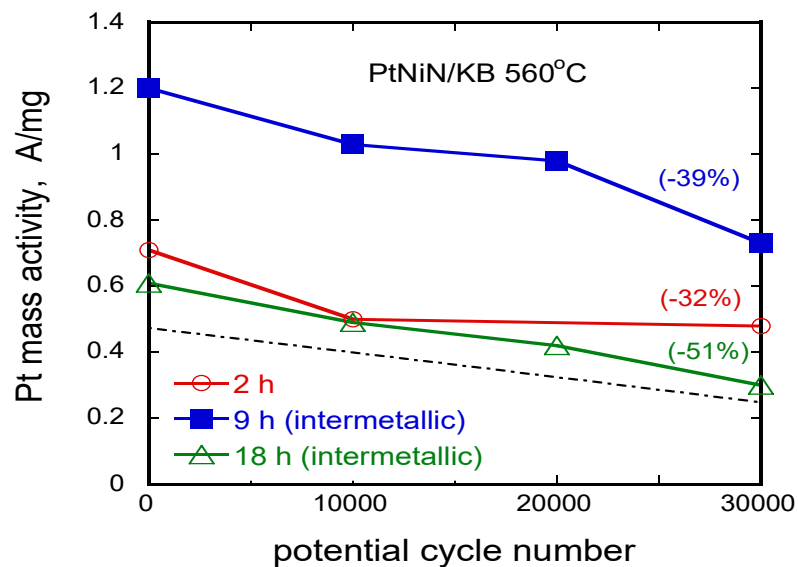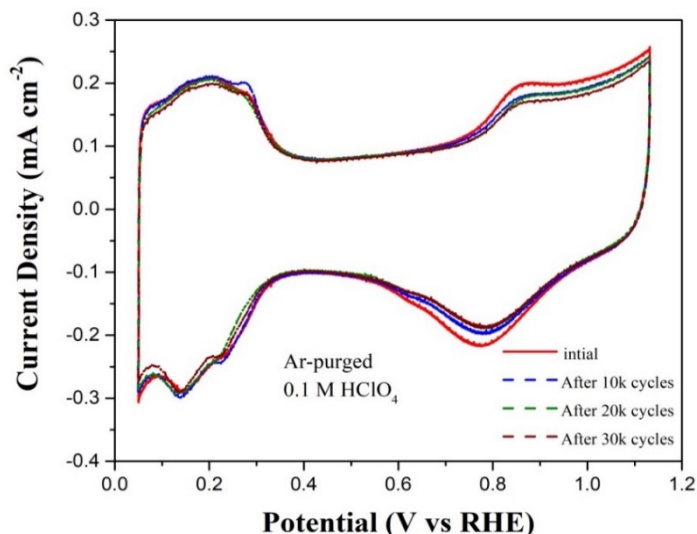
Pt mass activity ≥0.7 A/mg and ECSA >50 m^2/g after 30,000 cycles

Range of synthesis parameters narrowed down.

14

RDE screening PtNiN samples for MEA tests

y-axis left: $j_{0.9V}$ (A mg^{-1} Pt)
y-axis right: ECSA (m^2 g^{-1}Pt)
x-axis: Number of catalyst AST cycles

>0.6 A mg^{-1} >40 m^2 g^{-1}

Legend:
- ---○--- ---○--- PtNiN on KB
- ---■--- ---■--- PtNiN on VC
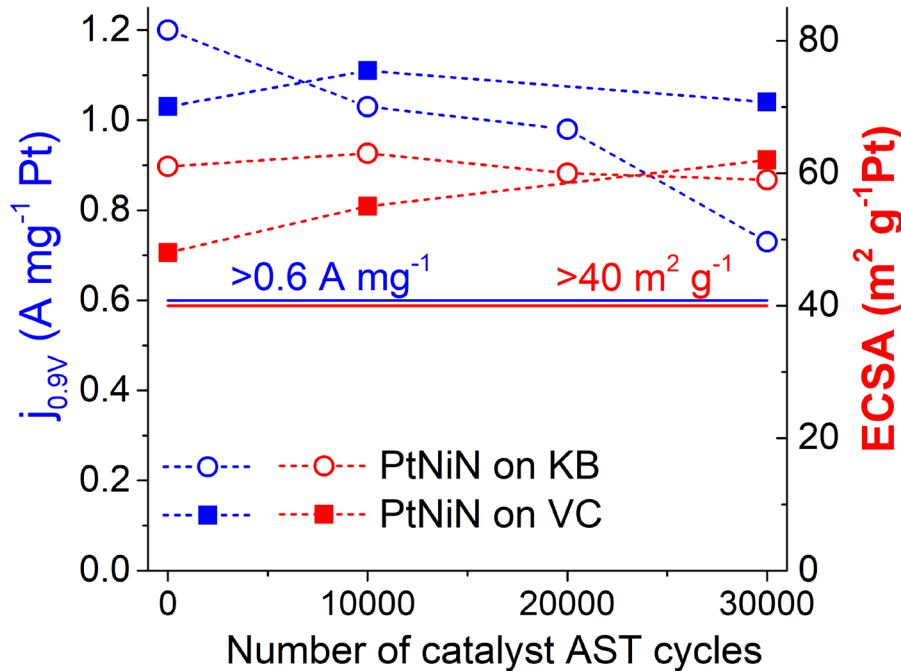
RDE screening criteria for PtNiN on VC and KB: **Activity >0.6 A/mg** and **ECSA > 40 m^2/g after catalyst AST on RDE**.

DOE target after catalyst AST: Activity >0.27 A/mg and ECSA loss <40%

Carbon effect found by MEA tests will guide future study for durability including support AST.

No loss of activity and ECSA for PtNiN on VC after catalyst and support ASTs on RDE at ambient temperature show promise to include support AST in MEA tests.

If the superior durability is confirmed in MEA tests, PtNiN will offer an opportunity for active bimetallic catalysts passing both catalyst and support ASTs.

15

3. Characterization of Pt-NbO$_x$C (KB600)

Pt-NbO$_x$C

Pt 4f$_{5/2}$ 74.1 eV

Pt 4f$_{7/2}$ 70.7 eV

Pt^{2+} 75.2 eV

Pt^{2+} 71.3 eV

XPS Intensity

80 78 76 74 72 70 68 66

Pt/C

Pt 4f$_{5/2}$ 74.8 eV

Pt 4f$_{7/2}$ 71.3 eV

Pt^{2+} 76.7 eV

Pt^{2+} 72.2 eV

XPS Intensity /a.u.

80 78 76 74 72 70 68 66

Binding Energy / eV

a

5 nm

Pt shells (ordered) on top of NbO$_x$ (amorphous) cores that are partly embedded in carbon

b

2 nm

c

Pt

d

Nb
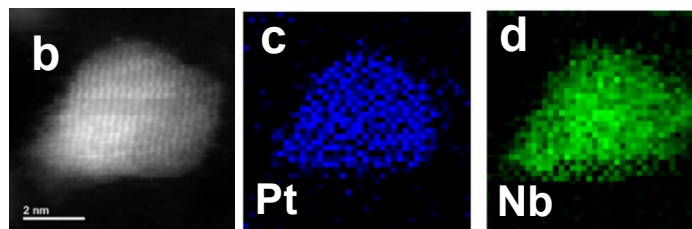
EELS mapping of Pt and Nb elements of a single particle
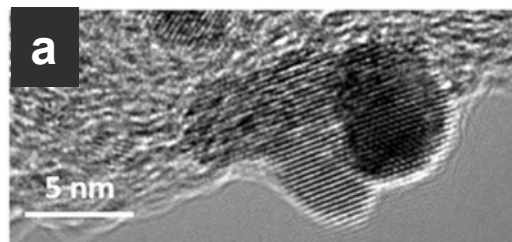
a

before

20 nm

b

after

20 nm

No significant change in particle size and density after durability tests.
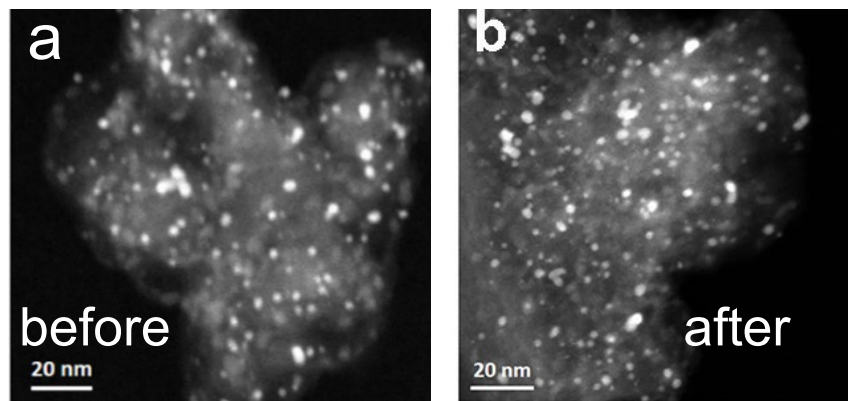
The 0.6 eV shift of XPS peak suggest partial charge transfer for NbO$_x$ to Pt, supporting that Pt is in contact with NbO$_x$.

KB600 can eliminate particles larger than 5 nm, but disappointing MEA results suggested that NbO$_x$ oxidation under fuel cell operating conditions were not fully prevented.

No go with NbO$_x$. Nb nitrides and porous carbon will be used in future research.

Proposed Future Work

Remaining challenges:

MEA validation and optimization need to be completed

Synthesis of PtNiN on corrosion-resistant supports

Future work

➢ Further optimization based on feedback of MEA tests and explore more favorable structure and synthesis methods

➢ Explore approaches for making highly active nitride catalysts on corrosion-resistant support to meet durability requirement for catalyst and support AST concurrently.

Any proposed future work is subject to change based on funding levels

Responses to Previous Year Reviewers' Comments

Comments:

Demonstrated improved durability and PGM activity with stable metal nitride, phosphide, and oxide cores on RDE results, but have not fully validated in MEA.

Need more structural characterization and fundamental understanding

Validating the performance of PtNiN in MEA should be a top priority.

Response:

RDE served as fast screening method for exploring new materials/structures. Out of five types of catalysts, PtNiN was selected for further development and validation in MEA.

Structural analysis clarified the benefits of nitriding and guided synthesis studies for further improving PtNiN catalysts.

Major effort and progress were made in establishing correlation between key structural parameters and catalytic performance, which ensured high quality of samples for MEA tests.

Samples were delivered to GM. MEA tests will be conducted in May and optimization will follow.

Collaboration

University and institution collaborators

BNL: Dong Su, Lijun Wu and Yimei Zhu, Xueru Zhao

High resolution TEM images and element mapping

University of Waterloo: Zhongwei Chen and Zhong Ma

Pt-NbO$_x$C synthesis and characterization

Korean Institute for Energy Research: Gu-Gon Park

Facilities at BNL

Center for Functional Nanomaterials

National Synchrotron Light Source (II)

Industrial collaborators

General Motor: Anu Kongkanand and Yun Cai   MEA tests

Toyota Motor: Hisao Kato

N.E. Chemcat: Hiroshi Igarashi and Kiyotaka Nagamori

Summary

Relevance

 Aiming at concurrently meeting activity targets at 0.9 V and at high current densities and durability targets after catalyst and support ASTs

Approach

 Exploring low-PGM or PGM-free core materials and novel core-shell structures using economically viable synthesis methods

Accomplishments

- Clarified beneficial effect of nitriding for PtNi bimetallic nanocatalysts
- Illustrated the advantages of Pt skin catalyst with bimetallic nitride core, Pt_{ML}-$[(PtNi)_4N]_{core}$.
- Several grams of PtNiN samples made with VC and KB as supports delivered for MEA tests.
- RDE tests showed that PtNiN likely to be more stable than PtNi and more active than PtCo.

Proposed future research

- Optimize PtNiN based on feedback of MEA tests by GM
- Synthesize active PtNiN with corrosion-resistant supports to achieve durability targets against ASTs for catalyst and support

Technical Back-Up Slides

RDE Testing Protocols (0.1 M HClO$_4$ solutions)

ECSA measured by average of H adsorption and desorption charges (Q- + Q+)/2/0.21, where Q- and Q+ are integration of negative and positive currents after subtracting double layer currents.

ORR polarization taken in positive sweep at 10 mV s^{-1}, 1600 rpm, iR-corrected using HFR near 0.4 V.

AST for Catalyst: 0.6 V (3s) – 0.95 V (3s) with 700 mV/s sweep rate between 0.6 and 0.95
AST for support: 1.0 - 1.5 V at 500 mV/S

MYRDD Table 3.4.7 Technical Targets: Electrocatalysts for Transportation Applications		
Characteristic	**Units**	**2020 Target**
PGM content at rated power	g$_{PGM}$/kW$_{gross}$ at 150 kPa (abs)	0.125
PGM loading	mg$_{PGM}$/cm^2 total	0.125
Mass activity	A/mgPGM at 900 mV$_{iR-free}$	0.44
Electrocatalyst stability (0.6 $\leftrightarrow$ 0.95 V)	% mass activity loss after 30K cycles	<40
Loss at 0.8 A/cm^2 (0.6 $\leftrightarrow$ 0.95 V)	mV loss after 30K cycles	<30
Support stability (1.0 $\leftrightarrow$ 1.5 V)	% mass activity loss after 5K cycles	<40
Loss at 1.5 A/cm^2 (1.0 $\leftrightarrow$ 1.5 V)	mV after 5K cycles	<30

In situ XAS of intermetallic PtNiN/KB at 560ºC in NH₃

Using our electrochemical cell with 1 M HClO4 at QAS beamline of NSLS-II
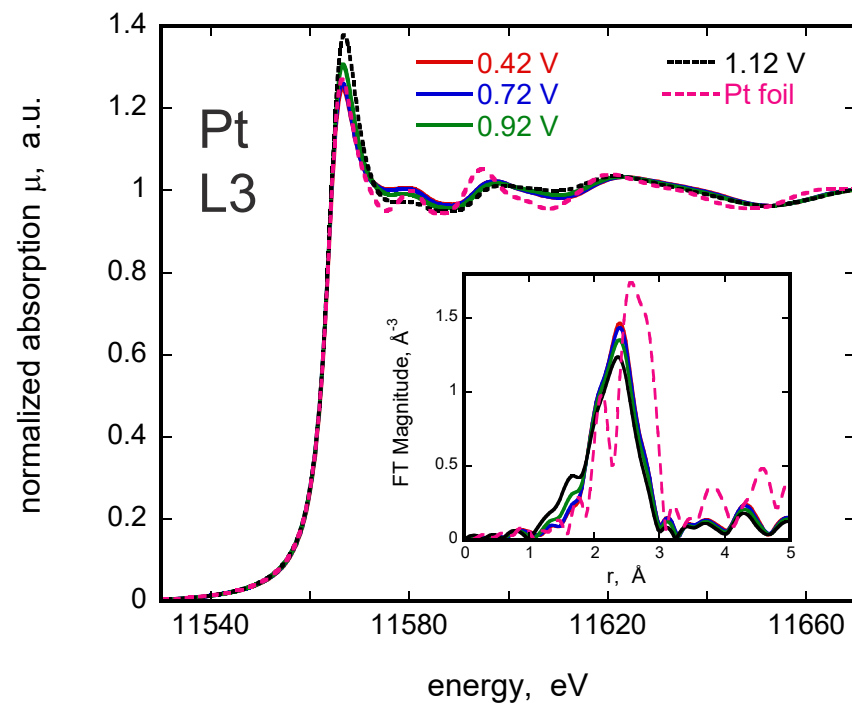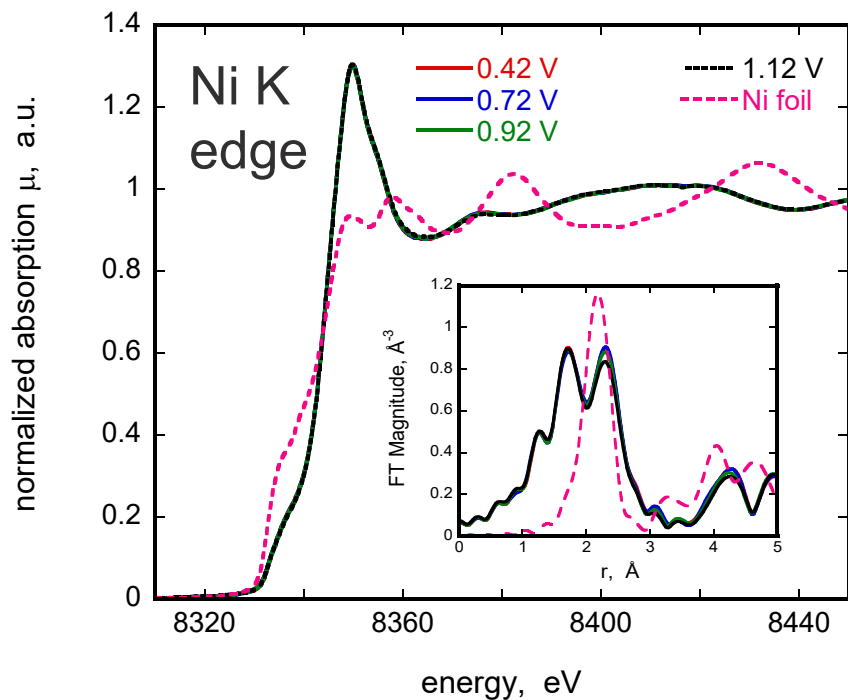
- ❑ No changes in Ni K edge spectra with increasing potentials from 0.42 V to 1.12 V, indicating that Ni is not oxidized due to protection of thin Pt shells, which is oxidized with increasing potentials as the white line intensity of Pt L3 spectra increases

- ❑ FT EXAFS of Ni K edge and Pt L3 from intermetallic PtNiN/KB catalysts show significant differences from their bulk structures. Detailed structural analysis is being made.